JOINT EUROPEAN TORUS

JET–P(89)30

E. Hinnov, B. Denne, TFTR Operating Team
and JET Team

Empirical Evaluation of 3-Electron QED Effects FRCM Lithium Like Resonance Lines of Elements Z=22-42 in the TFTR and JET Tokamaks

Empirical Evaluation of 3-Electron QED Effects FRCM Lithium Like Resonance Lines of Elements Z=22-42 in the TFTR and JET Tokamaks

E. Hinnov[1], B. Denne, TFTR Operating Team[1]
and JET Team*

JET-Joint Undertaking, Culham Science Centre, OX14 3DB, Abingdon, UK

[1]Plasma Physics Laboratory, Princeton University, Princeton, NJ 08543, U.S.A.
** See Appendix 1*

Preprint of Paper to be submitted for publication in
Physical Review A

Empirical Evaluation of 3-electron QED Effects from Lithiumlike Resonance Lines of Elements Z=22-42 in the TFTR and JET Tokamaks.

E. Hinnov and the TFTR Operating Team, Plasma Physics Laboratory,
Princeton University, Princeton N. J. 08543, U.S.A.
and
B. Denne and the JET Operating Team, JET Joint Undertaking,
Abingdon, OXON. OX14 3EA, U. K.

ABSTRACT

Most of the lithiumlike ion resonance line wavelengths have been remeasured relative to well-established lines of He II and C V, C VI in TFTR and to these are added the newly-measured lines of Kr XXXIV and Mo XL from JET, which allow a systematic evaluation of differences from calculated 1-electron Lamb-shift.

I. INTRODUCTION

The lithium sequence resonance lines, corresponding to the transitions $2s_{1/2}$ - $2p_{1/2}$ and $2s_{1/2}$ - $2p_{3/2}$ possess some unique advantages for the purpose of diagnosing tokamak-type plasmas. They are quite strong and relatively isolated from other lines of neighboring ionization stages of the same element. Their excitation potential, especially for heavier elements, is small compared to the ionization potential. As it is the ionization potential that principally determines the radial location of the ion, this means that the local electron

temperature is large compared to the excitation potential and hence the brightness of the lines is practically independent of the electron temperature in a given discharge, provided that it is high enough to produce the lithiumlike state. The latter condition implies that the central electron temperature, $T_e(0)$ satisfies

$$T_e(0) \approx E_i \gg E_x \tag{1}$$

with E_i and E_x the ionization potential of the lithiumlike state, and the excitation potential of the line, respectively.

Also, as it is usually the central or highest temperature ions that are of primary interest, Eq. (1) determines the element that is appropriate in a given tokamak discharge. Thus in the ST ("Symmetric Torus") tokamak, with $T_e(0) \sim 2$ keV, it was iron and chromium, in the PLT ("Princeton Large Torus") tokamak, with $T_e(0) \sim 2$ - 3 keV, it was nickel and copper, whereas TFTR ("Tokamak Fusion Test Reactor") has produced germanium and selenium in lithiumlike states, and the JET ("Joint European Torus") tokamak, with its large size and powerful r-f heating has been recently capable of raising molybdenum to the lithiumlike state[1].

While for plasma diagnostics, which depend on line intensity or Doppler shift measurements, the absolute accuracy of the wavelengths is not very important (about $\pm$ 0.1 - 0.3 Å is generally all that is required), these lithium sequence lines are also of vital interest to atomic physics, as is shown by a recent article by Johnson, Blundell and Sapirstein[2] and there measurement accuracy is at a premium. It is for this reason that we have made an effort to present our results with the maximum feasible precision, including also a reevaluation of our previous results with respect to better reference lines. We hope the present results will be of use for critical comparisons with theoretically calculated values.

II. EXPERIMENTAL RESULTS

The wavelengths of the lines up to selenium were measured in ohmically heated discharges of TFTR into which the appropriate element was injected by means of laser ablation. The krypton wavelengths were measured on the JET tokamak[3] into which krypton was admitted by means of a fast valve. The molybdenum was measured in JET plasmas heated by both ohmic current and r-f, by which means around 10 keV central electron temperature could be reached.

It is generally not difficult to identify the lithiumlike doublet, especially in the step-by-step fashion in which the experiments were performed. The wavelengths were measured by Schwob-Fraenkel spectrometers, which admit about 40 Å sections of the spectrum at a time, scanning this section repeatedly throughout the discharge. As wavelength standards we tried to use wherever possible the various orders of the resonance lines of C VI and C V, which are copiously emitted by these discharges, and are generally observable to 9th and 8th grating order, respectively.

For the wavelengths of the C V resonance and intercombination lines Edlén and Löfstrand[4] have given 40.2680 - 40.7306 Å, or the difference of 0.4626 Å. Although our measurements do not approach such accuracy, comparison of higher orders indicates consistently a wavelength difference $\sim$ 0.0003 Å smaller - except in the 5th order, where the intercombination line appears to be blended by something else. Accordingly, we have taken the resonance wavelength to be 40.2683 Å as may be consistent with the discussion by Edlén and Lõfstrand. Likewise, the second singlet line, observable in our spectra to third order, we have taken as 34.9728 Å. The iron, nickel, and titanium lines were remeasured in helium

discharges, using He II lines as references. The He II and C VI line wavelengths we use are those of Garcia and Mack[5].

The results of our measurements are given in Table I together with the estimated error limits. In almost all cases the line from $p_{1/2}$ was measurable with more precision in spite of its lower intensity and the fact that they were only measured in the first order, since the spectrometer wavelength coverage extends only to about 330 Å. This is because the quoted wavelengths depend rather critically on one or two reference wavelengths. Thus in Ti XX the $s_{1/2}$ - $p_{1/2}$ line is between the He II resonance line at 303.783 Å and a C IV line at 312.432 Å while the $s_{1/2}$ - $p_{3/2}$ depends mostly on C V in the 6th order - 241.610 Å, and the C VI line in 8th order - 269.888 Å. Also the $s_{1/2}$ - $p_{1/2}$ lines in Fe XXIV and Ni XXVI are accurately measured with respect to He II lines at 256.317 Å and 234.347 Å, respectively, while the $s_{1/2}$ - $p_{3/2}$ line of Fe XXIV was measured only relative to the O V triplet at 192.85 Å. The Ni XXVI $s_{1/2}$ - $p_{3/2}$ line is more fortunate - it is in the proximity of C VI in the 5th order at 168.680 Å. From Cu XXVII on, the $s_{1/2}$ - $p_{3/2}$ lines could be measured in second order and the Kr XXXIV in third order (while the second order was blended by the strong C VI n=2-3 complex at ~182.11 Å). Also the Mo lines could in principle be measured very accurately in higher orders but for the restrictions on machine time.

III. COMPARISON WITH CALCULATIONS

In Table II are given the wavenumbers for the $s_{1/2}$ - $p_{1/2}$ transition. The column marked σ_c shows the calculated values by Johnson *et al.*[2], which do not include the QED effects, and a number of these we have interpolated from their Table III. The column with σ_x shows the experimental wavenumbers together with the uncertainties as given in Table I, and Δ(c-x) is their difference that is presumably ascribable to the QED effects. The next column gives the one-electron Lamb-shift, as calculated by Johnson and Soff[6], with finite-nuclear-size corrections subtracted, as these are included[2] in the σ_c. Similar data for the $s_{1/2}$ - $p_{3/2}$ transition are presented in Table III.

The differences between the observed Δ(c-x) and the one-electron Lamb-shifts are presumably due to the screening of the Coulomb field of the nucleus by the 1s electrons. These differences are given in the last columns of Tables II and III and are shown graphically in Fig. 1 for the $s_{1/2}$ - $p_{1/2}$ transition, and Fig. 2 for $s_{1/2}$ - $p_{3/2}$.

The curve drawn in Fig. 1 is the weighted least squares fit to the data points. It has the equation

$$-\delta\sigma = 583.9 - 45.02Z + 1.666Z^2. \tag{2}$$

The uncertainties in the wavenumber differences diverge rather rapidly in Fig. 2, because of the short wavelengths of these lines. However, the straight line

$$-\delta\sigma = -598.0 + 41.81Z \tag{3}$$

shown in the Figure gives a reasonable fit to the data points.

Equations 2 and 3 may be extended slightly to higher Z-values with reasonable accuracy. We have therefore extended the interpolation of Tables II and III to Z=50, for the benefit

of future experiments. The corresponding wavelengths are given in Table IV.

We should also like to compare our present results with the extrapolated semiempirical values of Edlén[7]. As was noted in an earlier publication[8] based on poorer experimental data, there is evidence of a systematic deviation, in the sense of Edlén's wavelengths being increasingly too short at higher Z. Nevertheless his formulae are remarkably successful - even at molybdenum (Z=42) they predict wavelengths within 0.05 Å of our measured values.

ACKNOWLEDGEMENTS

We would like to thank Alan Ramsey and Brent Stratton at TFTR and George Magyar at JET for a variety of valuable contributions to this paper.

The close cooperation between the authors was made possible by several visits under the Large Tokamak Tripartite Agreement.

This work was partly supported by U. S. Department of Energy under contract no. DE-AC02-76-CHO-3073.

REFERENCES

1. B. Denne, G. Magyar and J. Jacquinot (to be published).

2. W. R. Johnson, S. A. Blundell, and J. Sapirstein, Phys. Rev. **A37**, 2764 (1988).

3. B. Denne, E. Hinnov, J. Ramette, and B. Saoutic (to be published).

4. B. Edlén and B. Löfstrand, J. Phys. B: At. Mol. Phys. **3**, 1380 (1970).

5. J. D. Garcia and J. E. Mack, J. Opt. Soc. Am. **55**, 654 (1965).

6. W. R. Johnson and G. Soff, At. Data and Nucl. Data Tables **33**, 405 (1985).

7. B. Edlén, Physica Scripta **28**, 51 (1983).

8. B. Denne and E. Hinnov, Physica Scripta **35**, 811 (1987).

TABLE I. Measured Wavelengths of the Lithium Sequence Resonance Lines in Å.

Ion	$\lambda(s_{1/2} - p_{1/2})$	$\lambda(s_{1/2} - p_{3/2})$	Source
Ti XX	309.065±0.015	259.300±0.02	TFTR
Cr XXII	279.729±0.02	223.010±0.02	TFTR
Fe XXIV	255.094±0.01	192.012±0.02	TFTR
Ni XXVI	234.155±0.01	165.396±0.01	TFTR
Cu XXVII	224.795±0.01	153.507±0.02	TFTR
Ge XXX	200.290±0.01	122.705±0.02	TFTR
Se XXXII	186.375±0.015	105.686±0.02	TFTR
Kr XXXIV	174.036±0.026	91.049±0.025	JET
Mo XL	143.998±0.02	58.499±0.02	JET

TABLE II. Calculated[a] (c) and experimental(x) wavenumbers (cm^{-1}) and their differences compared to the 1-electron QED effects, and the apparent screening by the 1s electrons, for the $2s_{1/2}$ - $2p_{1/2}$ transition.

Z	σ_c	σ_x	Δ(c-x)	1-el QED[b]	$-\delta\sigma_{1/2}$ (screening correction)
22	325707	323557±15	2150±15	2532	382±15
24	360463	357489±25	2974±25	3413	439±25
26	395945	392012±15	3933±15	4490	557±15
27	(413983)[c]	⟨409456⟩[d]	(4527)	5110	(583)
28	432233	427068±18	5165±18	5784	619±18
29	(450704)[c]	444850±20	5854±20	6522	668±20
30	469406	⟨462819⟩[d]	(6587)	7320	(733)
32	(507548)[c]	499276±25	8272±25	9116	844±25
34	(546738)[c]	536552±45	10185±45	11204	1018±45
36	587062	574594±85	12468±85	13598	1130±85
38	(628612)[c]	⟨613562⟩[d]	(15070)	16349	(1279)
40	(671486)[c]	⟨653479⟩[d]	(18007)	19456	(1449)
41	693452	⟨673741⟩[d]	(19711)	21250	(1539)
42	(715788)[c]	694454±96	21334±96	22956	1622±96
44	(761626)[c]	⟨736574⟩[d]	(25052)	26880	(1828)
45	(785154)[c]	⟨758063⟩[d]	(27091)	29023	(1932)
47	(833493)[c]	⟨802018⟩[d]	(31475)	33623	(2148)
50	(909384)[c]	⟨870395⟩[d]	(38989)	41487	(2498)

[a] Ref. 2

[b] Ref. 6, Table II less finite nuclear size effects.

[c] Our interpolations from Table III, Ref. 2.

[d] Interpolation from experimental data.

TABLE III. As Table II for the $2s_{1/2}$ - $2p_{3/2}$ transitions.

Z	σ_c	σ_x	Δ(c-x)	1-el QED[b]	$-\delta\sigma_{3/2}$ (screening correction)
22	387706	385654±30	2052±30	2346	294±30
24	451170	448410±40	2760±40	3152	392±40
26	524423	520800±55	3623±55	4133	510±55
27	(565299)[c]	⟨561135⟩[d]	(4164)	4695	(531)
28	609338	604610±36	4728±36	5308	580±36
29	(656801)[c]	651436±85	5365±85	5975	610±85
30	707964	⟨701300⟩[d]	(6664)	7320	(656)
32	(822559)[c]	814963±130	7596±130	8320	724±130
34	(955575)[c]	946199±180	9376±180	10199	823±180
36	1109688	1098310±300	11378±300	12353	975±300
38	(1287811)[c]	⟨1273994⟩[d]	(13817)	14808	(991)
40	(1493118)[c]	⟨1476605⟩[d]	(16513)	17587	(1074)
41	1607004	⟨1588921⟩[d]	(18083)	19199	(1116)
42	(1729001)[c]	1709431±585	19570±585	20711	1141±585
44	(1999182)[c]	⟨1976212⟩[d]	(22970)	24211	(1241)
45	(2148373)[c]	⟨2123533⟩[d]	(24840)	26123	(1283)
47	(2477592)[c]	⟨2448739⟩[d]	(28853)	30220	(1367)
50	(3057097)[c]	⟨3021360⟩[d]	(35736)	37228	(1492)

[b] Ref. 6, Table II less finite nuclear size effects.

[c] Our interpolations from Tables III and IV, Ref. 2.

[d] Interpolation from experimental data.

TABLE IV. Predicted wavelengths (in Å) for the lithiumlike doublet according to Eqs. 2,3 and the data in Tables II,III.

Z	$s_{1/2}$ - $p_{1/2}$	$s_{1/2}$ - $p_{3/2}$
38	162.983	78.493
40	153.027	67.723
41	148.425	62.936
44	135.764	50.602
45	131.915	47.091
47	124.686	40.837
50	114.890	33.098

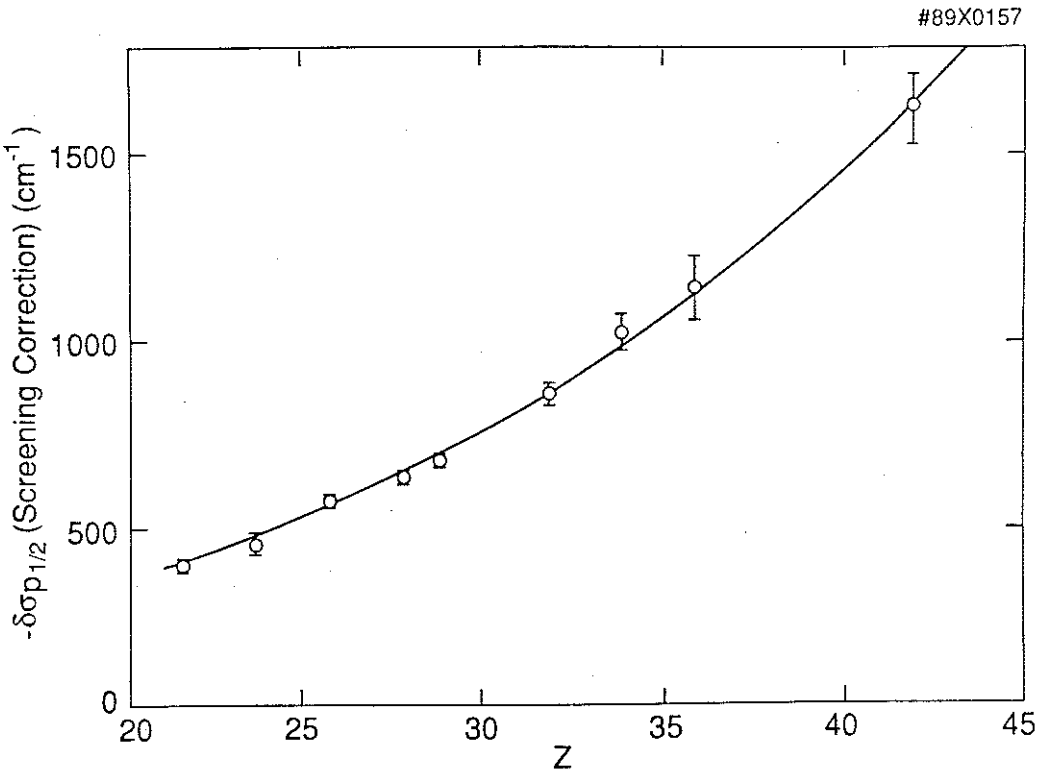

Fig. 1 The difference between the discrepancy of calculated and measured wavenumbers, $\Delta(c-x)$, and the calculated 1-electron QED effects vs. Z for the $s_{1/2}-p_{1/2}$ transitions. The continuous curve is Eq. 2.

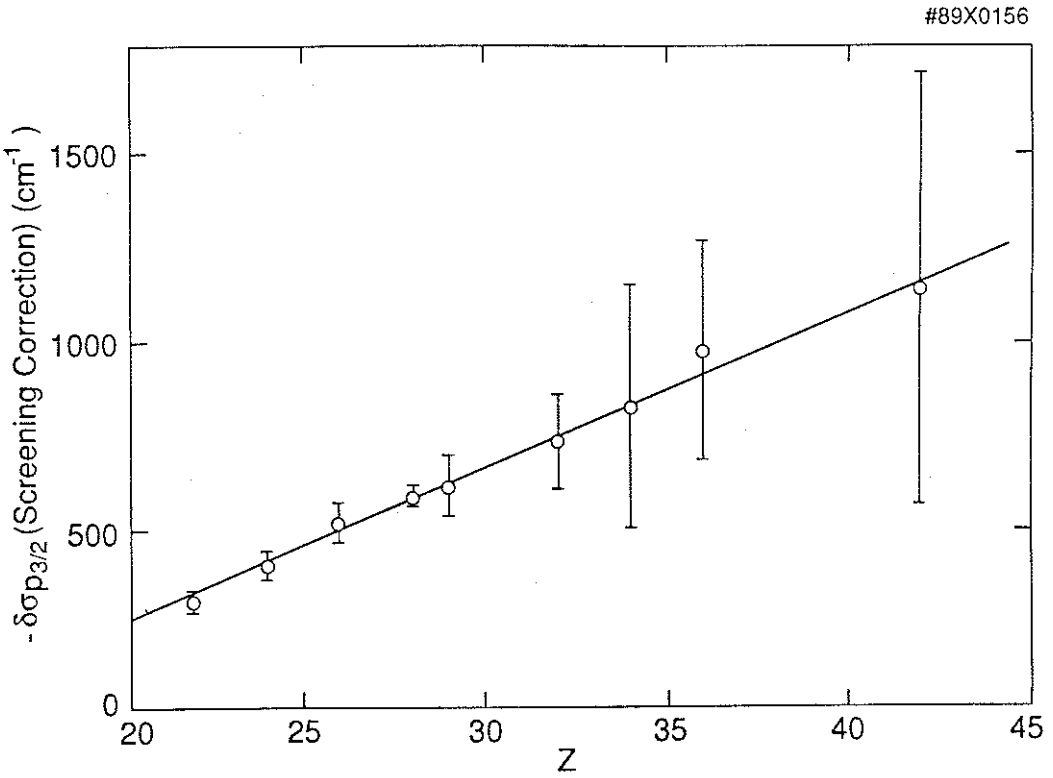

Fig. 2 As in Fig. 1 for the $s_{1/2}-p_{3/2}$ transitions. The straight line is Eq. 3.

APPENDIX 1.

THE JET TEAM

JET Joint Undertaking, Abingdon, Oxon, OX14 3EA, U.K.

J.M.Adams[1], F.Alladio[4], H.Altmann, R.J.Anderson, G.Appruzzese, W.Bailey, B.Balet, D.V.Bartlett, L.R.Baylor[24], K.Behringer, A.C.Bell, P.Bertoldi, E.Bertolini, V.Bhatnagar, R.J.Bickerton, A.Boileau[3], T.Bonicelli, S.J.Booth, G.Bosia, M.Botman, D.Boyd[31], H.Brelen, H.Brinkschulte, M.Brusati, T.Budd, M.Bures, T.Businaro[4], H.Buttgereit, D.Cacaut, C.Caldwell-Nichols, D.J.Campbell, P.Card, J.Carwardine, G.Celentano, P.Chabert[27], C.D.Challis, A.Cheetham, J.Christiansen, C.Christodoulopoulos, P.Chuilon, R.Claesen, S.Clement[30], J.P.Coad, P.Colestock[6], S.Conroy[13], M.Cooke, S.Cooper, J.G.Cordey, W.Core, S.Corti, A.E.Costley, G.Cottrell, M.Cox[7], P.Cripwell[13], F.Crisanti[4], D.Cross, H.de Blank[16], J.de Haas[16], L.de Kock, E.Deksnis, G.B.Denne, G.Deschamps, G.Devillars, K.J.Dietz, J.Dobbing, S.E.Dorling, P.G.Doyle, D.F.Düchs, H.Duquenoy, A.Edwards, J.Ehrenberg[14], T.Elevant[12], W.Engelhardt, S.K.Erents[7], L.G.Eriksonn[5], M.Evrard[2], H.Falter, D.Flory, M.Forrest[7], C.Froger, K.Fullard, M.Gadeberg[11], A.Galetsas, R.Galvao[8], A.Gibson, R.D.Gill, A.Gondhalekar, C.Gordon, G.Gorini, C.Gormezano, N.A.Gottardi, C.Gowers, B.J.Green, F.S.Griph, M.Gryzinski[26], R.Haange, G.Hammett[6], W.Han[9], C.J.Hancock, P.J.Harbour, N.C.Hawkes[7], P.Haynes[7], T.Hellsten, J.L.Hemmerich, R.Hemsworth, R.F.Herzog, K.Hirsch[14], J.Hoekzema, W.A.Houlberg[24], J.How, M.Huart, A.Hubbard, T.P.Hughes[32], M.Hugon, M.Huguet, J.Jacquinot, O.N.Jarvis, T.C.Jernigan[24], E.Joffrin, E.M.Jones, L.P.D.F.Jones, T.T.C.Jones, J.Källne, A.Kaye, B.E.Keen, M.Keilhacker, G.J.Kelly, A.Khare[15], S.Knowlton, A.Konstantellos, M.Kovanen[21], P.Kupschus, P.Lallia, J.R.Last, L.Lauro-Taroni, M.Laux[33], K.Lawson[7], E.Lazzaro, M.Lennholm, X.Litaudon, P.Lomas, M.Lorentz-Gottardi[2], C.Lowry, G.Magyar, D.Maisonnier, M.Malacarne, V.Marchese, P.Massmann, L.McCarthy[28], G.McCracken[7], P.Mendonca, P.Meriguet, P.Micozzi[4], S.F.Mills, P.Millward, S.L.Milora[24], A.Moissonnier, P.L.Mondino, D.Moreau[17], P.Morgan, H.Morsi[14], G.Murphy, M.F.Nave, M.Newman, L.Nickesson, P.Nielsen, P.Noll, W.Obert, D.O'Brien, J.O'Rourke, M.G.Pacco-Düchs, M.Pain, S.Papastergiou, D.Pasini[20], M.Paume[27], N.Peacock[7], D.Pearson[13], F.Pegoraro, M.Pick, S.Pitcher[7], J.Plancoulaine, J-P.Poffé, F.Porcelli, R.Prentice, T.Raimondi, J.Ramette[17], J.M.Rax[27], C.Raymond, P-H.Rebut, J.Removille, F.Rimini, D.Robinson[7], A.Rolfe, R.T.Ross, L.Rossi, G.Rupprecht[14], R.Rushton, P.Rutter, H.C.Sack, G.Sadler, N.Salmon[13], H.Salzmann[14], A.Santagiustina, D.Schissel[25], P.H.Schild, M.Schmid, G.Schmidt[6], R.L.Shaw, A.Sibley, R.Simonini, J.Sips[16], P.Smeulders, J.Snipes, S.Sommers, L.Sonnerup, K.Sonnenberg, M.Stamp, P.Stangeby[19], D.Start, C.A.Steed, D.Stork, P.E.Stott, T.E.Stringer, D.Stubberfield, T.Sugie[18], D.Summers, H.Summers[20], J.Taboda-Duarte[22], J.Tagle[30], H.Tamnen, A.Tanga, A.Taroni, C.Tebaldi[23], A.Tesini, P.R.Thomas, E.Thompson, K.Thomsen[11], P.Trevalion, M.Tschudin, B.Tubbing, K.Uchino[29], E.Usselmann, H.van der Beken, M.von Hellermann, T.Wade, C.Walker, B.A.Wallander, M.Walravens, K.Walter, D.Ward, M.L.Watkins, J.Wesson, D.H.Wheeler, J.Wilks, U.Willen[12], D.Wilson, T.Winkel, C.Woodward, M.Wykes, I.D.Young, L.Zannelli, M.Zarnstorff[6], D.Zasche[14], J.W.Zwart.

PERMANENT ADDRESS

1. UKAEA, Harwell, Oxon. UK.
2. EUR-EB Association, LPP-ERM/KMS, B-1040 Brussels, Belgium.
3. Institute National des Récherches Scientifique, Quebec, Canada.
4. ENEA-CENTRO Di Frascati, I-00044 Frascati, Roma, Italy.
5. Chalmers University of Technology, Göteborg, Sweden.
6. Princeton Plasma Physics Laboratory, New Jersey, USA.
7. UKAEA Culham Laboratory, Abingdon, Oxon. UK.
8. Plasma Physics Laboratory, Space Research Institute, Sao José dos Campos, Brazil.
9. Institute of Mathematics, University of Oxford, UK.
10. CRPP/EPFL, 21 Avenue des Bains, CH-1007 Lausanne, Switzerland.
11. Risø National Laboratory, DK-4000 Roskilde, Denmark.
12. Swedish Energy Research Commission, S-10072 Stockholm, Sweden.
13. Imperial College of Science and Technology, University of London, UK.
14. Max Planck Institut für Plasmaphysik, D-8046 Garching bei München, FRG.
15. Institute for Plasma Research, Gandhinagar Bhat Gujat, India.
16. FOM Instituut voor Plasmafysica, 3430 Be Nieuwegein, The Netherlands.
17. Commissiariat à L'Energie Atomique, F-92260 Fontenay-aux-Roses, France.
18. JAERI, Tokai Research Establishment, Tokai-Mura, Naka-Gun, Japan.
19. Institute for Aerospace Studies, University of Toronto, Downsview, Ontario, Canada.
20. University of Strathclyde, Glasgow, G4 ONG, U.K.
21. Nuclear Engineering Laboratory, Lapeenranta University, Finland.
22. JNICT, Lisboa, Portugal.
23. Department of Mathematics, Univeristy of Bologna, Italy.
24. Oak Ridge National Laboratory, Oak Ridge, Tenn., USA.
25. G.A. Technologies, San Diego, California, USA.
26. Institute for Nuclear Studies, Swierk, Poland.
27. Commissiariat à l'Energie Atomique, Cadarache, France.
28. School of Physical Sciences, Flinders University of South Australia, South Australia SO42.
29. Kyushi University, Kasagu Fukuoka, Japan.
30. Centro de Investigaciones Energeticas Medioambientales y Techalogicas, Spain.
31. University of Maryland, College Park, Maryland, USA.
32. University of Essex, Colchester, UK.
33. Akademie de Wissenschaften, Berlin, DDR.

CR 88.49.1A